Characterization of Endophilin B1b, a Brain-specific Membrane-associated Lysophosphatidic Acid Acyl Transferase with Properties Distinct from Endophilin A1*

Jan Modregger‡§, Anne A. Schmidt¶, Brigitte Ritter‡||, Wieland B. Huttner**‡‡, and Markus Plomann‡§§

*From the ‡Center for Biochemistry II, Medical Faculty, Joseph-Stelzmann-Strasse 52, University of Cologne, Cologne D-50931, Germany, the ¶Institut de Biologie Physico-Chimique, Unité Propre de Recherche CNRS 1929, 13 rue Pierre et Marie Curie, Paris 75005, France, and the **Max-Planck-Institute of Molecular Cell Biology and Genetics, Pfotenhauerstrasse 108, Dresden D-01307, Germany*

We have characterized mammalian endophilin B1, a novel member of the endophilins and a representative of their B subgroup. The endophilins B show the same domain organization as the endophilins A, which contain an N-terminal domain responsible for lipid binding and lysophosphatidic acid acyl transferase activity, a central coiled-coil domain for oligomerization, a less conserved linker region, and a C-terminal Src homology 3 (SH3) domain. The endophilin B1 gene gives rise to at least three splice variants, endophilin B1a, which shows a widespread tissue distribution, and endophilins B1b and B1c, which appear to be brain-specific. Endophilin B1, like endophilins A, binds to palmitoyl-CoA, exhibits lysophosphatidic acid acyl transferase activity, and interacts with dynamin, amphiphysins 1 and 2, and huntingtin. However, in contrast to endophilins A, endophilin B1 does not bind to synaptojanin 1 and synapsin 1, and overexpression of its SH3 domain does not inhibit transferrin endocytosis. Consistent with this, immunofluorescence analysis of endophilin B1b transfected into fibroblasts shows an intracellular reticular staining, which in part overlaps with that of endogenous dynamin. Upon subcellular fractionation of brain and transfected fibroblasts, endophilin B1 is largely recovered in association with membranes. Together, our results suggest that the action of the endophilins is not confined to the formation of endocytic vesicles from the plasma membrane, with endophilin B1 being associated with, and presumably exerting a functional role at, intracellular membranes.

The endophilins, originally named SH3p4/p8/p13 (1–3), SH3GL1–3 (4), and SH3d2a-c (5), are a family of proteins identified in search for SH3 domain-containing proteins. The most extensively studied isoform of the mammalian endophilins, the neuron-specific endophilin A1 (2, 6), is essential for synaptic vesicle endocytosis (7–12). Via its C-terminal SH3 domain, endophilin A1 binds to proline-rich domains of amphiphysin (13), dynamin (2), and synaptojanin (2, 3), three proteins also involved in synaptic vesicle endocytosis (14).

In addition to interacting with other proteins, endophilin A1 has been shown to bind lipids. Thus, endophilin A1 binds to lysophosphatidic acid (LPA)[1] and fatty acyl-CoA and, via its intrinsic lysophosphatidic acid acyl transferase (LPA-AT) activity, condenses them to phosphatidic acid (8). Moreover, endophilin A1 binds to liposomes and alone is sufficient to deform them into narrow tubules (15). The latter observation provides direct evidence in support of the hypothesis that the role of endophilin A1 in synaptic vesicle endocytosis is related to its ability to generate membrane curvature (6, 8, 9, 15, 16).

In contrast to the neuron-specific isoform endophilin A1, another member of the endophilins A, endophilin A2, shows a ubiquitous tissue distribution (2, 4). Accordingly, the endophilins A have been implicated not only in synaptic vesicle endocytosis but in various membrane traffic events, most of which, however, occur at the plasma membrane (7–12, 17–20). We report here the molecular and cell biological characterization of a novel endophilin that is a representative of a new subgroup of endophilins, the endophilins B (6). While sharing many structural and functional properties with the endophilins A, endophilin B is distinct in that it does not appear to operate in endocytosis at the plasma membrane but, rather, is associated with intracellular membranes. While this work, which focuses on the brain-specific splice variant endophilin B1b, was prepared for publication, other investigators independently reported on other members of the endophilins B, which show a widespread tissue distribution (15, 21, 22).

EXPERIMENTAL PROCEDURES

Yeast Two-hybrid Screen

The experiments were performed using the Matchmaker 2 two-hybrid system (Clontech). The full-length PACSIN 1 open reading frame

was cloned in-frame with the GAL4 DNA-binding domain in the pAS2–1 vector and confirmed by sequencing. The pAS2–1 PACSIN 1 plasmid was sequentially cotransformed with the Matchmaker mouse brain cDNA library into the yeast strain Y190. Transformed yeast cells expressing interacting Gal4 fusion proteins were selected by the ability to grow on minimal synthetic dropout medium lacking L-tryptophan, L-leucine, and L-histidine and checked for their ability to express the *lacZ* gene by β-galactosidase filter assays. Positive clones were isolated by re-streaking and growth on cycloheximide-containing medium and verified for the interaction with PACSIN 1 by mating with Y187 yeast cells transformed with pAS2–1 PACSIN 1. Plasmid DNA of positive clones was isolated and sequenced in both directions with universal and internal primers using the ABI Prism Big Dye Terminator Cycle Sequencing Ready Reaction kit, and products were resolved on an ABI Prism 377 automated sequencer (PerkinElmer Life Sciences/Applied Biosystems). DNA and protein sequence analyses were performed using the GCG software package (University of Wisconsin, Madison, WI), and multiple gene databases were searched using BLAST programs (23).

Isolation of Clones and DNA Analysis

Four filters with dotted cDNA derived from a 9-day postcoitum murine embryo cDNA library (no. 559) were obtained from the Resource Center of the German Human Genome Project. Filter hybridization was performed in 50% formamide, 5× Denhardt's solution (0.1% bovine serum albumin, 0.1% Ficoll 400, and 0.1% polyvinylpyrrolidone), 5× SSPE (0.75 M NaCl, 50 mM sodium phosphate (pH 7.6), and 5 mM EDTA), 1.5% SDS, and 300 μg/ml salmon sperm DNA with a 1831-bp probe specific for murine endophilin B1. The latter cDNA fragment was derived from the two-hybrid clone by *Eco*RI/*Xho*I digestion and radiolabeled by random priming (TaKaRa). The filters were finally washed with 0.1× SSC (15 mM NaCl, 1.5 mM sodium citrate, pH 7.5) and 0.1% SDS at 65 °C for 20 min and subjected to autoradiography. Positive clones and protein sequence analyses were performed as described above.

RT-PCR and Southern Blot Analysis

Reverse transcription of poly(A)$^+$ RNA isolated from various mouse tissues was performed with Superscript II (Promega) according to the manufacturer's protocol. For each tissue tested 500 ng of poly(A)$^+$ RNA was converted into first-strand cDNA using oligo(dT) primers in a 10-μl reaction mix. Endophilin B1 fragments were amplified by PCR using AmpliTaq DNA Polymerase (PerkinElmer Life Sciences) and specific primers (sense: 5'-AGA CTG GAT TTG GAT GCT GC-3', antisense: 5'-AGG TCA TTG AGG TTA GAA GG-3'). The resulting PCR fragments were separated by electrophoresis on a 4% TBE polyacrylamide gel and blotted onto a Hybond XL membrane (Amersham Biosciences) by electrophoretic transfer (200 mA, 4 h) in 0.5× TBE (24). Hybridization was performed in a formamide mix with a radiolabeled probe corresponding to nucleotides 1–1831 of mouse endophilin B1b generated by using a labeling kit (TaKaRa). The blot was stringently washed and analyzed using autoradiography.

Antibodies

A GST murine endophilin B1b fusion protein was produced by cloning the cDNA corresponding to the C-terminal 201 amino acids (residues 186–386) into the pGEX-4T1 vector (Amersham Biosciences) followed by expression in *Escherichia coli* (BL21). The fusion protein was purified by affinity chromatography on glutathione-Sepharose 4B (Amersham Biosciences) and used as an antigen to immunize rabbits. Polyclonal antibodies against amphiphysin 2/BIN1 (EVA) were a generous gift of Dr. Pietro De Camilli (Yale University, New Haven, CT), and antibodies against synaptojanin 1 (1852) were a generous gift from Dr. Peter McPherson (McGill University, Montreal, Canada). Polyclonal antibodies against synapsin 1 were purchased from Sigma, monoclonal antibodies against dynamin (clone 41) were from Transduction Laboratories, a monoclonal antibody against huntingtin was from Chemicon, a monoclonal antibody against amphiphysin 1 (clone 2) was from Oncogene Research Products, and a monoclonal antibody against the hemagglutinin (HA) tag was from Roche Molecular Biochemicals. All monoclonal antibodies were derived from mouse except for anti-HA, which was from rat. For visualization of primary antibodies Alexa 488- and Cy3-conjugated goat antisera against rabbit and mouse immunoglobulins (IgG) were purchased from Molecular Probes and Jackson ImmunoResearch Laboratories, respectively.

Immunoblotting

Proteins were extracted by mechanical disruption of freshly prepared mouse tissues or NIH 3T3 cells in radioimmune precipitation assay buffer (150 mM NaCl, 1% Nonidet P-40, 0.5% sodium deoxycholate, 0.1% SDS, 50 mM Tris/HCl, pH 7.5) containing protease inhibitors (Sigma, 50 μl per gram of tissue) and subsequent centrifugation to remove detergent-insoluble material. Aliquots of the extracts corresponding to 80 μg of protein were resolved on 10% SDS-polyacrylamide gels followed by transfer to PVDF membranes (Millipore). Blots were blocked at room temperature for 1 h with 5% skim milk in TBS containing 0.1% Tween 20 (TBST), rinsed with TBST, and incubated at room temperature for 1 h with diluted antibodies. After three 5-min washes with TBST, bound antibodies were detected using peroxidase-conjugated anti-rabbit IgG antibodies (Dako) and the ECL kit (Amersham Biosciences).

Protein Binding to Endophilins

Bead-immobilized Endophilins—GST fusion proteins of full-length murine endophilin B1b, full-length murine endophilin A1 (8), and a C-terminal fragment of murine endophilin A3 (2) were bound to glutathione-Sepharose 4B (Amersham Biosciences) in PBS. Mouse brains were homogenized on ice in 2.5 ml/g wet weight PBS containing 1% deoxycholate supplemented with a protease inhibitor mixture (Sigma, 50 μl per gram of tissue) using a Dounce homogenizer and centrifuged for 30 min at 21,000 × *g*. The supernatant was decanted and recentrifuged. After addition of Triton X-100 to a final concentration of 0.05% to the supernatant, it was dialyzed against PBS buffer lacking deoxycholate for 48 h. Glutathione-Sepharose 4B beads saturated with GST-endophilins were incubated overnight with supernatant containing 1 mg of the protein extract in 400 μl at 4 °C with end-over-end rotation. The beads were washed extensively with PBS/1% Triton X-100. Bound proteins were eluted with double-concentrated SDS-PAGE sample buffer, separated by SDS-PAGE on a 4–10% gradient gel, and transferred to a PVDF membrane for subsequent immunodetection.

Endophilin Overlay—PVDF membranes containing rat brain proteins were prepared as described above for immunoblotting, blocked, rinsed with TBST, and incubated for 12 h at 4 °C with GST fusion proteins containing the murine endophilin B1 and rat endophilins A1–A3 SH3 domains. The latter were produced by cloning the cDNAs corresponding to the C-terminal SH3 domains into the pGEX-6p1 vector (Amersham Biosciences) followed by expression in *E. coli* (BL21) and purification by affinity chromatography on glutathione-Sepharose 4B (Amersham Biosciences). Following incubation with the GST fusion proteins, the membranes were washed three times for 5 min, and bound GST fusion proteins were detected using an anti-GST antibody (Amersham Biosciences), peroxidase-conjugated anti-rabbit IgG secondary antibodies (Dako), and the ECL kit (Amersham Biosciences).

Subcellular Fractionation

The complete open reading frame of murine endophilin B1b was cloned into the eukaryotic expression vector pHA-CMV (Clontech). NIH 3T3 cells were transfected with HA-tagged endophilin B1b using FuGENE 6 (Roche Molecular Biochemicals) according to the manufacturer's protocol, and subcellular fractions were prepared essentially as described previously (25). All steps were performed at 4 °C. The cell pellet was homogenized in 3 ml of ice-cold 0.32 M sucrose in 5 mM HEPES (pH 7.4) supplemented with a protease inhibitor mixture (Sigma), using nine strokes of a glass homogenizer. The homogenate was centrifuged for 10 min at 1000 × *g* to produce a pellet (P1), which was washed by resuspension in an equal volume of homogenization buffer and recentrifuged for 10 min at 1000 × *g*. The original supernatant and wash were combined (S1) and then centrifuged at 10,000 × *g* for 20 min yielding pellet (P2) and supernatant (S2). The S2 fraction was centrifuged at 105,000 × *g* for 60 min to give a high speed pellet (P3) and a high speed supernatant (S3). The subcellular fractions obtained by this method were analyzed by Western blotting.

For the isolation and analysis of membrane fractions derived from mouse brain, a discontinuous sucrose gradient was used (26). All steps were performed at 4 °C. Finely chopped mouse brains were homogenized in 3 ml per gram of wet weight of ice-cold 0.25 M sucrose in 10 mM Tris-HCl (pH 7.4) supplemented with a protease inhibitor mixture (Sigma), using ten strokes of a glass homogenizer. Larger cell debris and nuclei were removed by centrifugation for 10 min at 500 × *g*. After adjusting the post-nuclear supernatant to 1.4 M sucrose and 1 mM neutralized EDTA, 3 ml of the post-nuclear supernatant were underlaid with 2.5 ml of 1.6 M sucrose/10 mM Tris-HCl (pH 7.4) and overlaid with 4 ml of 1.2 M sucrose/10 mM Tris-HCl (pH 7.4) and 2.5 ml of 0.8 M sucrose/10 mM Tris-HCl (pH 7.4). After centrifugation at 110,000 × *g* for 2 h, the various sucrose phases, interfaces, and the pellet were collected for analysis by immunoblotting.

Immunofluorescence

NIH 3T3 fibroblasts plated on 12-mm glass coverslips were transfected with the pHA-endophilin B1b expression vector using FuGENE 6 (Roche Molecular Biochemicals) according to the manufacturer's protocol. 24 h after transfection, cells were fixed in 2% paraformaldehyde in PBS for 10 min, permeabilized by incubation in 0.2% Triton X-100 in PBS for 1 min, and blocked for 15 min in 1% bovine serum albumin and 5% horse serum in PBS. All antibody incubations and washing steps were performed in PBS containing 0.02% Triton X-100. Samples were analyzed by confocal laser scanning microscopy (Leica).

Endocytosis Assay

For flow cytometric analysis (FACS) of transferrin uptake, NIH 3T3 cells were transfected with constructs containing the C-terminal SH3 domain of either murine endophilin A1, A2, or B1 fused to red fluorescence protein (DsRed), and with DsRed as negative control (27). 48 h after transfection, cells were incubated for 20 min in serum-free medium followed by a 30-min incubation in medium containing 5% fetal calf serum and 25 μg/ml FITC-conjugated human transferrin (Molecular Probes), washed three times in PBS, trypsinized with 1% trypsin, and finally washed once with PBS. A FACSCalibur (Becton Dickinson) was used to detect red fluorescence proteins (FL2) and FITC-transferrin (FL1) in 0.5–1.0 $\times$ 10^4 cells.

Palmitoyl-CoA Binding Assay

NIH 3T3 fibroblasts were transfected with HA-tagged endophilin B1b and harvested after 48 h. Cells were lysed in ice-cold PBS containing 0.1% Triton X-100, followed by short sonication, and the lysates were centrifuged 20 min at 20,000 $\times$ g in a cooled centrifuge. The supernatants were incubated with 50 μl of palmitoyl-CoA-agarose (Sigma) overnight by end-over-end rotation at 4 °C, centrifuged for 5 min at 500 $\times$ g to remove unbound proteins, washed three times with PBS/0.1% Triton X-100, and eluted with 4 mM free palmitoyl-CoA in PBS/0.1% Triton X-100 or with 1% Triton X-100 in PBS. Aliquots of the lysates, bound and unbound material, supernatants, and the eluates were analyzed by SDS-PAGE followed by immunoblotting using HA high affinity antibodies coupled to horseradish peroxidase (Roche Molecular Biochemicals).

LPA-AT Assay

Recombinant murine endophilin B1b was produced by cloning the cDNA corresponding to the full-length protein into the pGEX-6P1 vector (Amersham Biosciences) followed by expression in *E. coli* (BL21) and purification according to the manufacturer's instructions with the following modifications. The bacterial pellet was resuspended in PBS, incubated on ice for 20 min in the presence of lysozyme (20 mg/ml), sonicated, and incubated at 4 °C for another 20 min after adding Triton X-100 to a final concentration of 1%. After centrifugation of the lysate at 20,000 $\times$ g for 15 min and of the resulting supernatant at 226,000 $\times$ g for 1 h, glutathione-Sepharose 4B was added to the high speed supernatant followed by incubation for 4 h at 4 °C. GST fusion protein bound to the Sepharose was washed twice with PBS containing 1% Triton X-100 followed by three additional washes using PBS without detergent. For the LPA-AT assay, either the GST fusion protein or endophilin B1b without GST tag was used. In the first case, GST-endophilin B1b and, as control, GST were eluted according to the manufacturer's protocol. In the second case, endophilin B1b was liberated from GST by proteolytic cleavage with the PreScission protease (Amersham Biosciences). Recombinant His-tagged mouse endophilin A1 was expressed and purified by poly(L-proline) affinity chromatography from the 280,000 $\times$ g supernatant obtained from bacteria lysed by freezing/thawing in the absence of detergent, as previously described (8).

For the data shown in Fig. 5*B*, the LPA-AT activity of endophilins was determined as described previously (8). For the data shown in Fig. 5*C*, the LPA-AT activity of endophilins was determined by modifying the previously described assay (8) as follows. Aliquots of [^{14}C]oleoyl-CoA (100 nCi, 56 mCi per mmol, PerkinElmer Life Sciences) in 0.01 M sodium acetate buffer, pH 6, were dried in a SpeedVac and dissolved by adding 100 μl of gel-filtered cytosol (GGA buffer) followed by sonication for 2 min. The tubes were then transferred to ice and brought to a final reaction volume of 150 μl by sequential additions of GGA buffer, LPA, and recombinant proteins. LPA was added from a 1 mM stock prepared in LPA buffer (20 mM HEPES-KOH, pH 7.4, 10 mM sucrose, 1 mM EDTA, 2.5 mg/ml fatty acid-free bovine serum albumin (Roche Molecular Biochemicals)) to a final concentration of 10 μM. For the incubations that did not contain LPA, an equivalent volume of LPA buffer was added. Recombinant endophilins A1 and B1 were added at a final

concentration of 500 nM. Reactions were carried out for 20 min at 37 °C and terminated by addition of 150 μl ice-cold 0.8 M KCl, 0.2 M H$_3$PO$_4$. Samples were mixed with 450 μl of chloroform/methanol (2:1) and centrifuged for 5 min at 10,000 $\times$ g. The lower phase was collected, dried, redissolved in 35 μl of chloroform/methanol/water (2:1:0.1, v/v), subjected (along with a [^{14}C]phosphatidic acid standard, PerkinElmer Life Sciences) to thin layer chromatography using Silica Gel 60 and chloroform/pyridine/formic acid (50:30:7, v/v) as solvent, and analyzed by phosphorimaging.
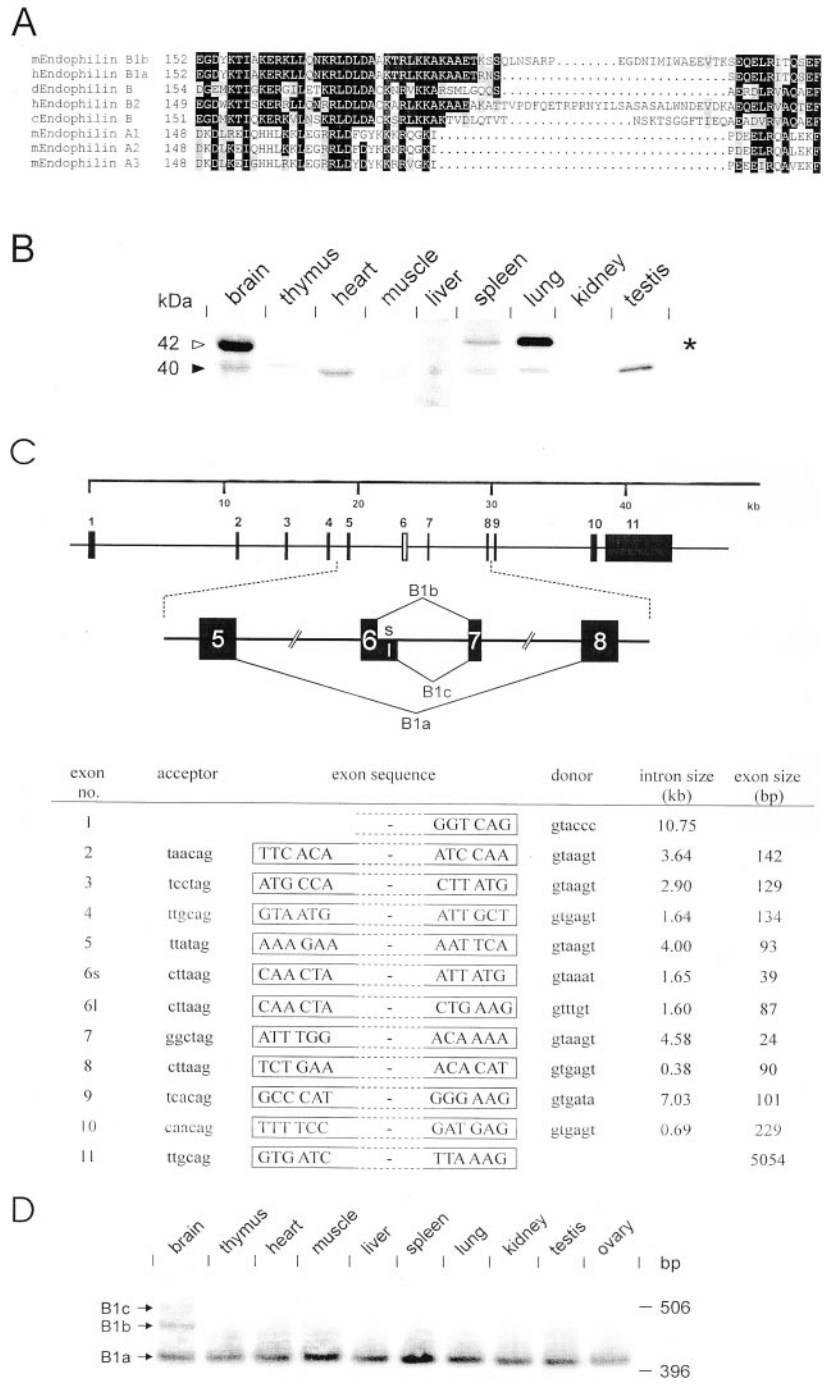
RESULTS

Isolation and Characterization of Endophilin B1 cDNAs—In a search for PACSIN 1/syndapin 1 (28, 29) interaction partners using the yeast two-hybrid system, we identified one false-positive clone (see explanation below) that represented a novel endophilin distantly related to the endophilins A. We therefore further characterized this protein and named it endophilin B1 to distinguish it from the previously known members, which we propose to refer to as endophilins A1–A3 (6). Using the two-hybrid clone as a probe, we obtained three clones on screening a mouse embryo cDNA library. Two contained the entire coding region (nucleotides 271–1431) and comprised a cDNA of endophilin B1 with a length of 4012 bp. The first in-frame ATG is located 271 nucleotides from the 5′-end and fulfills Kozak's criteria for a translation initiation site, showing conservation of 9 out of 10 bases in the consensus (30). In the mouse mRNA this putative initiator is not preceded by any in-frame stop codons, which in the two-hybrid system leads to the translation of additional 90 amino acids, including several prolines. These were sufficient to interact with the PACSIN 1 SH3 domain, resulting in the false-positive interaction (data not shown). In human endophilin B1, whose cDNA sequence was obtained from data base searches and sequencing of EST clones, the putative translation initiation site is located at nucleotides 151–153 and, in contrast to the murine homolog, is preceded by an in-frame stop codon (nucleotides 70–72).

The predicted protein products encoded by the open reading frames range from 365 to 386 residues in length, with calculated molecular masses of 40,855 to 43,239 Da. Reasons for the differences in length include the existence of splice variants such as endophilins B1a and B1b (Fig. 1*A*), which are addressed further below. The human and murine endophilin B1 sequences show 96% amino acid identity to each other, and the murine protein is 58% identical to the *Drosophila melanogaster* homolog CG9834 (EMBL accession number AJ437142) (11) and 48% identical to the *Caenorhabditis elegans* homolog F35A5–8 (GenBank™ accession number U46675). The comparison of murine endophilin B1 to endophilins A1–3 revealed an average overall identity of only 25%, showing that endophilin B1 is only distantly related to the endophilin A subfamily and, together with endophilin B2, which originally was referred to as SH3GLB2 (21), belongs to a novel endophilin subfamily whose overall domain organization is, however, the same as that of the endophilins A. Specifically, we noticed the highest similarity of endophilin B1 to the endophilins A in (i) the N-terminal domain (38–42%), being the region of LPA acyl transferase activity, liposome binding, and tubulation (8, 15), (ii) the central coiled-coil region (41–52%), and (iii) the C-terminal SH3 domain (46–48%). Following our deposition of the mouse and human endophilin B1 sequences in the data base in 2000 as cited in a previous study (6), three other groups have independently reported sequences identical to endophilin B1a (15, 21, 22), the short splice variant of endophilin B1, which, in contrast to the brain-specific longer splice variant endophilin B1b studied here, shows a widespread tissue distribution (see below).

Expression and Genomic Organization of the Endophilin B1 Gene—To determine the expression of the endophilin B1 gene, we performed Northern blot analysis on mRNA isolated from

A

B

FIG. 1. **Genomic organization, splice variants, and tissue distribution of endophilin B1.** *A*, sequence comparison of the exon 6- and 7-containing region of murine (*m*) endophilin B1b (accession number AF272946) with human (*h*) endophilin B1a (accession number AF263293), *Drosophila* (*d*) endophilin B1 (accession number AE003796), human endophilin B2 (SH3GLB2, accession number BC014635 (21)), *C. elegans* (*c*) endophilin B1 (F35A5–8, accession number U46675), and the murine endophilins A1, A2, and A3 (accession numbers U58886, U58885, and U58887, respectively). Identical amino acids are shown with a *black background*, and conservative substitutions, as defined by the BoxShade program, are *gray*. Gaps in the sequences, needed to optimize the alignment, are represented by *dots*. *B*, Western blot of adult murine total tissue protein (80 μg per lane) using an antiserum against the recombinant C-terminal half of murine endophilin B1b. *Open arrowhead*, endophilin B1b (42 kDa); *filled arrowhead*, endophilin B1a (40 kDa); *asterisk*, additional endophilin B1 splice variant (43 kDa) distinct from endophilin B1b (see "Results" and Fig. 1*D*). *C*, genomic structure of human endophilin B1, showing the position and size of the exons (*black bars* and *boxes*) as well as several splice variants. Endophilin B1a lacks exons 6 and 7; endophilins B1b and B1c contain both these exons, but endophilin B1b uses a splice site within exon 6, *i.e.* contains a short version of exon 6 (6s), whereas endophilin B1c contains the long version of exon 6 (6l). The table lists the exon-intron boundary sequences and the size of the known exons and introns. *D*, RT-PCR using primers in exons 5 and 10 and poly(A)$^+$ RNA isolated from various mouse tissues. Note the widespread tissue distribution of endophilin B1a and the brain-specific expression of endophilins B1b and B1c.

C

exon no.	acceptor	exon sequence		donor	intron size (kb)	exon size (bp)
1		-	GGT CAG	gtaccc	10.75	
2	taacag	TTC ACA -	ATC CAA	gtaagt	3.64	142
3	tcctag	ATG CCA -	CTT ATG	gtaagt	2.90	129
4	ttgcag	GTA ATG -	ATT GCT	gtgagt	1.64	134
5	ttatag	AAA GAA -	AAT TCA	gtaagt	4.00	93
6s	cttaag	CAA CTA -	ATT ATG	gtaaat	1.65	39
6l	cttaag	CAA CTA -	CTG AAG	gttttgt	1.60	87
7	ggctag	ATT TGG -	ACA AAA	gtaagt	4.58	24
8	cttaag	TCT GAA -	ACA CAT	gtgagt	0.38	90
9	tcacag	GCC CAT -	GGG AAG	gtgata	7.03	101
10	cancag	TTT TCC -	GAT GAG	gtgagt	0.69	229
11	ttgcag	GTG ATC -	TTA AAG			5054

D

several adult mouse tissues. This revealed a similar tissue distribution of endophilin B1 mRNAs as previously reported (22) (data not shown). Four mRNA transcripts were detected, with sizes of 2.6, 5.0, 6.5, and 8.0 kb. Most of these can be attributed to the alternative use of polyadenylation signals, as can be concluded from the existence of various endophilin B1 expressed sequence tags (ESTs) and numerous potential polyadenylation sites in the murine and human 3′-noncoding region (data not shown).

A rabbit antiserum raised against the GST-endophilin B1 fusion protein recognized a band of 40 kDa in most tissues tested, referred to as endophilin B1a (Fig. 1*B*, *filled arrowhead*) but also reacted with a larger, 42-kDa form of the protein specifically detected in brain tissue and referred to as endophilin B1b (Fig. 1*B*, *open arrowhead*). In addition, an immunoreactive band of 43 kDa was detected in lung and to lesser extent

in spleen (Fig. 1*B*, *asterisk*). The identity of these different forms of endophilins B will be discussed below.

To explore whether endophilins B1a and B1b represented alternatively spliced variants, we performed a sequence search against the high throughput genomic sequences data base and identified the human endophilin B1 gene-containing genomic clone J612B15, which was mapped to the chromosomal region 1p22.2–1p31.1 by the Sanger Centre. By comparing it with the human and murine cDNAs, we defined the exon/intron boundaries of all 11 exons of the endophilin B1 gene, except for the 5′-end of exon 1. This showed that the ubiquitously expressed endophilin B1a (Fig. 1*B*, *filled arrowhead*) represents a splice variant lacking exons 6 and 7 (Fig. 1*C*). Using RT-PCR analysis with primers in exons 5 and 10, we verified the existence of two additional transcripts, endophilins B1b and B1c, that appear to be brain-specific (Fig. 1*D*). Endophilin B1b uses a donor splice

site within exon 6 and therefore contains the shorter exon 6s and exon 7 (Fig. 1*C*). Endophilin B1c, which exists as a brain-derived EST clone (GenBank[TM] accession number BF470089), contains the longer exon 6l and exon 7. The extended exon 6l leads to the insertion of 16 additional amino acids. Here, the alternative splice site within exon 6 is not used (Fig. 1*C*). This indicates that in brain, exons 6s, 6l, and 7 are alternatively used. Presumably, the 43-kDa endophilin B1 variant in lung and spleen (see Fig. 1*B*, *asterisk*) represents yet another splice variant not detected by the oligonucleotides used.

Protein Interactions of Endophilin B1—To gain insight into the function and mechanism of action of endophilin B1, we analyzed its possible interaction with dynamin, huntingtin, synaptojanin, and amphiphysin, which were previously shown to bind to endophilins A (2, 13, 31). For this purpose, a mouse brain detergent extract was incubated with bead-immobilized GST fusion proteins containing full-length mouse endophilin B1b, endophilin A1, a C-terminal endophilin A3 fragment (2), or, as a control, GST alone. Brain was chosen because this tissue expresses several splice variants of endophilin B1 (see Fig. 1, *B* and *D*) and therefore is likely to contain relevant interaction partners. Endophilin B1 was able to bind dynamin, huntingtin, and both amphiphysins as detected by immunoblotting (Fig. 2*A*). Compared with endophilins A1 and A3, endophilin B1 preferentially bound the larger splice variant of amphiphysin 2. Interestingly, endophilin B1, in contrast to endophilins A1 (2) and A3, did not bind to synaptojanin 1, which has been implicated in synaptic vesicle uncoating (32). We also investigated the possible interactions of endophilins A and B with synapsin 1, which has been proposed to anchor the reserve pool of synaptic vesicles via binding to actin (reviewed in Ref. 33). Remarkably, synapsin 1 was detected among the proteins bound to GST-endophilin A1 and A3 but not GST-endophilin B1 (Fig. 2*A*).

Endophilin B1, like the endophilins A, contains a single SH3 domain, which is likely to be responsible for these protein interactions. We therefore further analyzed some of the interactions in an overlay assay by incubating blots containing brain proteins with purified GST-SH3-domain fusion proteins (Fig. 2*B*). Interestingly, the SH3 domain of endophilin B1, like that of endophilins A1–3, recognized dynamin (Fig. 2*B*, *filled circles*), amphiphysin 1 (Fig. 2*B*, *filled squares*), and amphiphysin 2 (Fig. 2*B*, *open circles*), whereas synaptojanin 1 was only recognized by the SH3 domain of endophilins A but not endophilin B1 (Fig. 2*B*, *open squares*). The interaction of the SH3 domains of endophilins A with synapsin 1 in the overlay assay was at the limits of detection (data not shown). These observations confirm the results obtained with the bead-immobilized GST-endophilin fusion proteins (Fig. 2*A*) and show that the binding of dynamin and amphiphysins 1 and 2 to bead-immobilized endophilin B1b involves the direct interaction of its SH3 domain with the former three proteins.

Using the yeast two-hybrid system, we could verify the direct interaction of endophilin B1b with dynamin and huntingtin and show that its SH3 domain was sufficient for this interaction (data not shown). In these studies, we also noticed that full-length endophilin B1b can self interact, in contrast to an endophilin B1b deletion construct lacking the N-terminal LBM (lipid binding and modifying) domain and the coiled-coil region (data not shown). The ability of the coiled-coil region to mediate homo-oligomerization of the endophilins B has also been described by others (21).

Intracellular Localization of Endophilin B1b—The subcellular localization of endophilin B1b was studied by both subcellular fractionation and immunofluorescence (Fig. 3). For this purpose, we engineered a hemagglutinin (HA) epitope-tagged
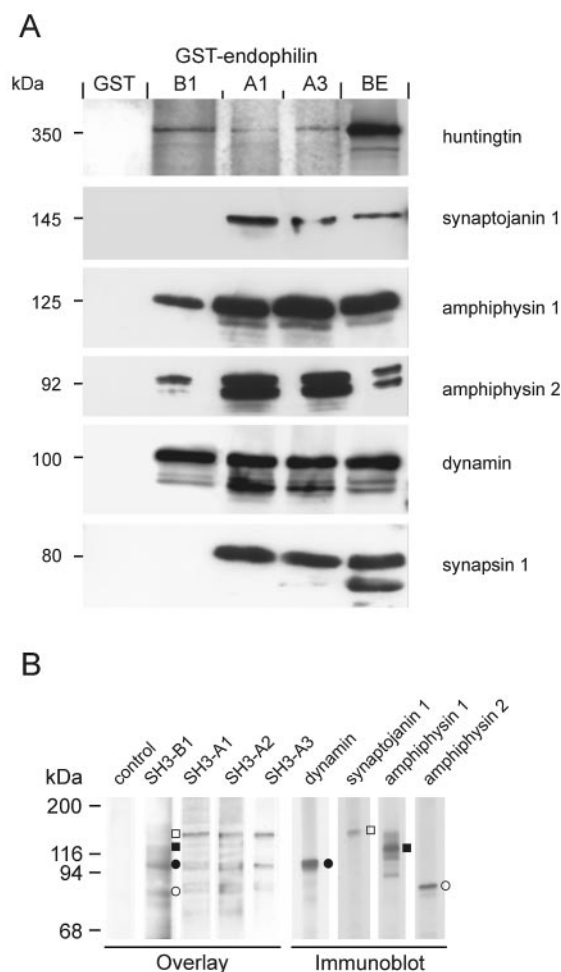

Fig. 2. **Protein interactions of endophilin B1.** *A*, a mouse brain detergent extract was incubated with immobilized GST fusion proteins of mouse endophilins B1b, A1, and A3, as well as GST as control. Bound proteins were analyzed by immunoblotting. *BE*, an aliquot of the brain extract used as starting material. Longer exposure of the synaptojanin and synapsin immunoblots (comparable to the amphiphysin immunoblots) did not yield detectable signals for endophilin B1 (data not shown). *B*, proteins in a rat brain detergent extract were separated by SDS-PAGE and blotted on PVDF membrane. Stripe aliquots of the blot were incubated (i) either with GST (control) or GST fusion proteins containing the SH3 domain of endophilin B1 (*SH3-B1*) or endophilins A1–3 (*SH3-A1/2/3*), followed by detection of bound GST fusion protein by immunoblotting using anti-GST antibody (*Overlay*); (ii) or with antibodies against the indicated proteins (*Immunoblot*). *Open squares*, synaptojanin; *filled squares*, amphiphysin 1; *filled circles*, dynamin; *open circles*, amphiphysin 2.

version of endophilin B1b. Upon differential centrifugation of transfected NIH 3T3 cells, virtually all of HA-endophilin B1b was recovered in the microsomal pellet (*P3*) and was not detectable in the crude nuclear pellet (*P1*), the crude mitochondrial fraction (*P2*), nor the cytosol (*S3*) (Fig. 3*A*, *upper panel*).

To complement these results, a postnuclear supernatant of a mouse brain homogenate was subjected to floatation/sedimentation using a discontinuous sucrose gradient (26) (Fig. 3*A*, *lower panel*). The vast majority of endophilin B1 floated from the 1.4 M sucrose load to fractions of lower density, indicating its association with membranes. The splice variant endophilin B1c, which was only detected in brain by RT-PCR (Fig. 1*D*), was detected only at the 0.8 M/1.2 M sucrose interface (Fig. 3*A*, *lower panel*, *diamond*). Endophilin B1b, like endophilin B1c brain-specific (Fig. 1, *B* and *D*) and the major splice variant in this tissue (Fig. 1*B*), peaked at the 0.8 M/1.2 M sucrose interface but was also found in the 1.2 M sucrose fraction and in the 1.4 M sucrose load (Fig. 3*A*, *lower panel*, *open arrowhead*). Consist-

A

B

FIG. 3. **Subcellular localization of endophilin B1b.** *A*, subcellular fractions from NIH 3T3 cells transiently transfected with HA-tagged endophilin B1b were obtained by differential centrifugation and analyzed by Western blotting using an antibody against the HA tag of endophilin B1 (*upper panel*). A post-nuclear supernatant of mouse brain was subjected to discontinuous sucrose gradient centrifugation, and the fractions were analyzed by Western blotting using antibodies against endophilin B1 (*lower panel*). The molarity of the various sucrose phases and interfaces is indicated. *P*, pellet. *Open arrowhead*, endophilin B1b (42 kDa); *filled arrowhead*, endophilin B1a (40 kDa); *diamond*, additional endophilin B1 splice variant, presumably endophilin B1c. *B*, NIH 3T3 cells transiently transfected with HA-tagged endophilin B1b were analyzed by double immunofluorescence using an antibody against the HA tag (*green*, *left panel*) and antibody recognizing endogenous dynamin (*red*, *middle panel*).
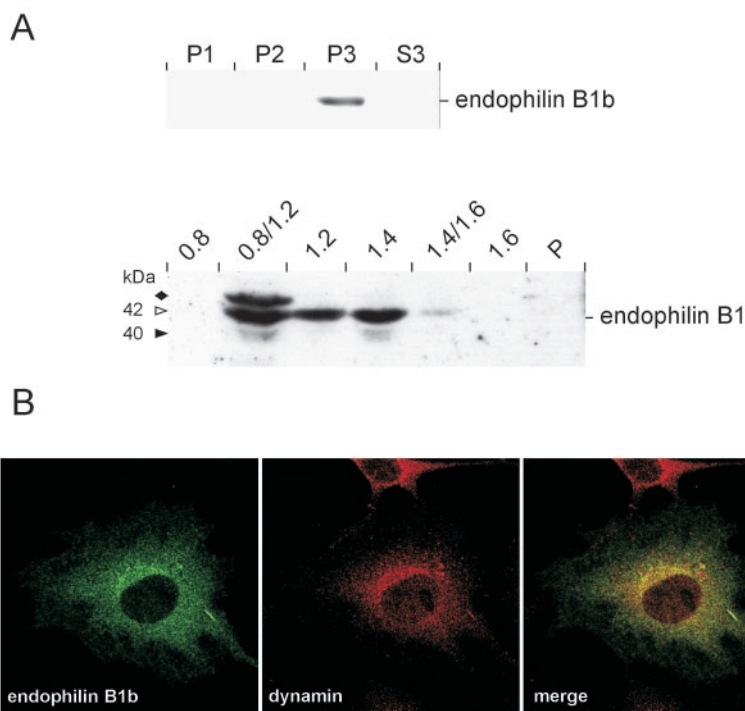
ent with the immunoblotting results using total brain extract (Fig. 1*B*), only a weak signal was obtained for the shortest endophilin B1 splice variant, the ubiquitous endophilin B1a, which was detected at the 0.8 M/1.2 M sucrose interface and in the 1.4 M sucrose load (Fig. 3*A*, *lower panel*, *filled arrowhead*).

To obtain a first indication as to the membranes with which endophilin B1 is associated, HA-tagged endophilin B1b expressed in NIH 3T3 cells was analyzed by confocal immunofluorescence microscopy. The transfected endophilin B1b showed a reticular pattern throughout the cytoplasm, indicating its association with intracellular membranes rather than the plasma membrane (Fig. 3*B*). Part of the HA-endophilin B1b staining appeared to overlap with that of endogenous dynamin (presumably dynamin 2) (Fig. 3*B*).

Lack of Influence of Endophilin B1 Overexpression on Endocytosis—The SH3 domain of endophilin A1 was previously shown to inhibit transferrin endocytosis (17). We analyzed the SH3 domain of endophilin B1 fused to the red fluorescent protein DsRed for a similar activity by transiently overexpressing it in NIH 3T3 cells, with the SH3 domains of endophilin A1 and A2 fused to DsRed as positive controls and DsRed alone as negative control. Cells showing DsRed fluorescence were isolated by FACS, and their uptake of FITC-labeled transferrin was quantified (Fig. 4). In contrast to cells expressing the SH3 domain of endophilins A1 and A2, which showed an inhibition of transferrin uptake as expected from previous studies (17), no inhibition of endocytosis was observed in cells expressing the SH3 domain of endophilin B1 (Fig. 4).

Endophilin B1 Binds Activated Fatty Acids and Exhibits LPA Acyl Transferase Activity—We examined whether endophilin B1, like endophilin A1 (8), binds fatty acyl-CoA and exhibits LPA-AT activity. NIH 3T3 cells were transiently transfected with HA-tagged murine endophilin B1b. As revealed by Western blotting (Fig. 5*A*), HA-endophilin B1b present in a detergent extract prepared from the cells efficiently bound to palmitoyl-CoA agarose and was eluted by addition of excess free palmitoyl-CoA.

To analyze its potential LPA-AT activity, we expressed murine endophilin B1b as a GST fusion protein in bacteria. Because GST-endophilin B1b was purified from bacteria lysed in
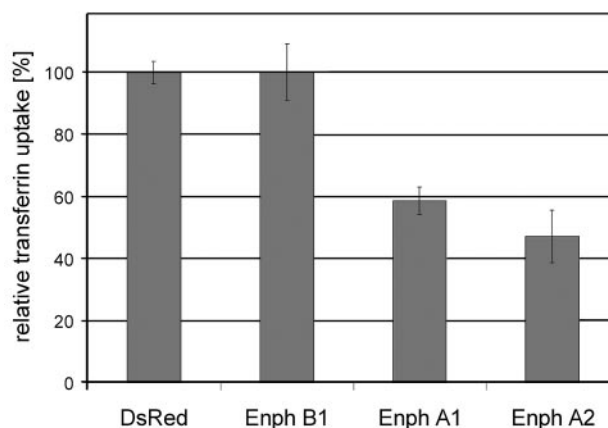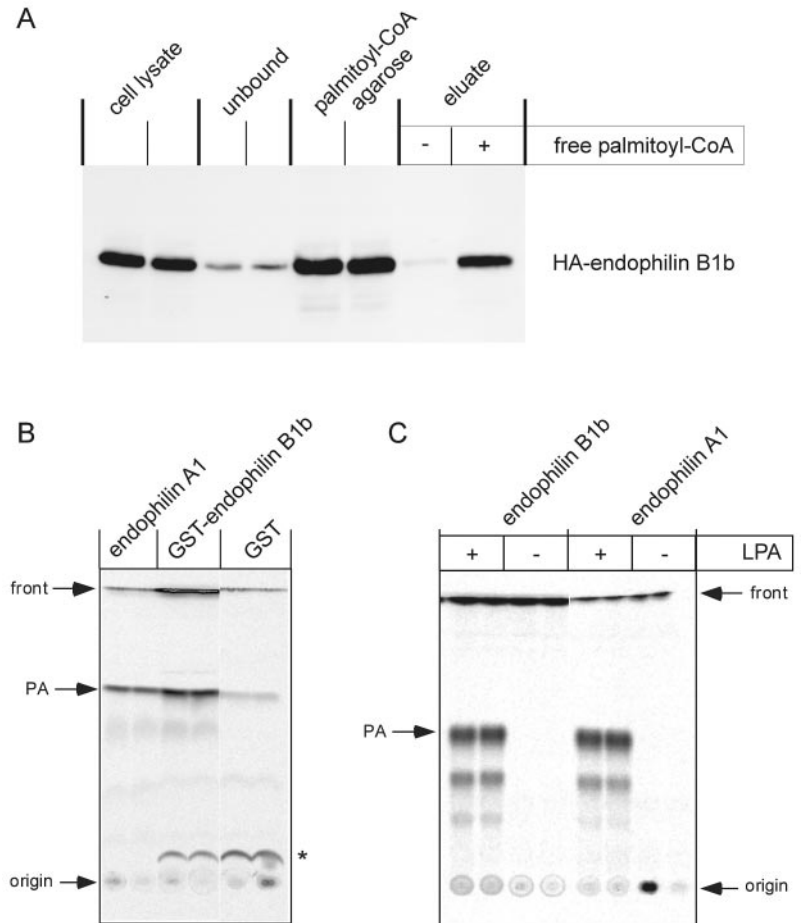

FIG. 4. **Transferrin uptake of endophilin SH3-domain-transfected cells.** NIH 3T3 cells were transiently transfected with the SH3-domain of mouse endophilin A1, A2, and B1, each fused to DsRed, or with DsRed alone as control. FITC-transferrin uptake of DsRed-expressing cells was quantitated by FACS and is expressed as the percentage of that observed for control cells. The values are the mean of three independent experiments; *bars*, ± S.D.

the presence of detergent, we first compared its LPA-AT activity with that of GST alone, purified in parallel by glutathione-Sepharose affinity chromatography. The latter control should provide an indication of the amount of endogenous bacterial LPA-AT activity that was nonspecifically present in the glutathione-Sepharose eluate because of the use of detergent. Indeed, the GST control sample showed some background LPA-AT activity (Fig. 5*B*). However, the LPA-AT activity of GST-endophilin B1b was substantially higher than that of the GST control and in the range of His-tagged mouse endophilin A1 purified by poly(L-proline) affinity chromatography from bacteria lysed in the absence of detergent (8) (Fig. 5*B*). The LPA-AT activity of purified endophilin B1b liberated from GST by specific proteolytic cleavage, like that of purified His-tagged mouse endophilin A1, was totally dependent on the presence of exogenously added LPA, with the level of LPA-AT activity of the two endophilins being very similar (Fig. 5*C*).

DISCUSSION

The present characterization of endophilin B1, a representative of the B subgroup of the endophilins (6), suggests that the role of the endophilins in membrane dynamics is broader than previously assumed. Endophilin B1 has the same overall domain organization as the previously characterized endophilins A, with the hallmarks of an N-terminal lipid binding and modifying domain (LBM domain (11)), and a C-terminal SH3 domain mediating protein interaction (see below). Like endophilin A1 (8, 15, 16), endophilin B1 binds lipids, exhibits LPA-AT activity, and tubulates liposomes, properties that have been shown or are likely to reside in its LBM domain (Fig. 5) (15). Despite these common properties, the sequence homology in the LBM domain between endophilin B1 and endophilin A1 is significantly less than that between the endophilins A. This should facilitate the identification of amino acid residues that are of critical importance for the LPA-AT activity and liposome tubulation of the endophilins, such as phenylalanine 10 in endophilin A1 whose hydrophobic nature has been shown to be crucial for liposome binding and tubulation (15).

However, in contrast to endophilin A1, which is essential for synaptic vesicle endocytosis from the plasma membrane (7–12), and endophilin A2, which has been implicated in the formation of tubular plasma membrane invaginations at podosomes of non-neuronal cells (20), endophilin B1 expressed in non-neuronal cells does not appear to be involved in endocytosis at the plasma membrane (Fig. 4) but, rather, is associated with intracellular membranes (Fig. 3), suggesting a role in intracellular membrane dynamics. Consistent with this, the protein interaction partners of endophilin B1 are not identical to those of endophilin A1. On the one hand, endophilin B1, like endophilin A1 (2), directly interacts via its SH3 domain with dynamin

(Fig. 2), whose various isoforms and splice variants have been implicated in membrane tubulation and vesicle formation not only from the plasma membrane but also from intracellular membranes (34, 35). On the other hand, however, in contrast to endophilin A1, endophilin B1 does not bind to synaptojanin 1 and synapsin 1 (Fig. 2), which have been implicated specifically in the membrane dynamics of synaptic vesicles (14, 33).

Another direct interaction partner of endophilin B1, huntingtin (Fig. 2), deserves special comment. Huntingtin is a protein of unknown function that has been reported to be associated with vesicles in neuronal cell bodies and dendrites (36, 37). At the trans-Golgi network and endosomes, huntingtin has been detected on both clathrin-coated and non-coated vesicles and buds (38). Endophilin A3 was previously identified as an interaction partner of huntingtin, specifically the Huntington's disease exon 1 protein containing the pathogenic glutamine repeat (31). Because endophilin A3 was reported to promote the formation of insoluble polyglutamine-containing aggregates *in vivo* and, therefore, hypothesized to be involved in the progressive pathology of Huntington's disease, it will be of interest to determine whether the same is true for endophilin B1.

The conclusion that the endophilins have a broader role in membrane dynamics than previously assumed is also supported not only by the existence of a second endophilin B gene, endophilin B2 (21), but also by the presence of several endophilin B1 transcripts resulting from alternative use of polyadenylation signals and alternative splicing (Fig. 1). These transcripts yield endophilin B1 variants with a widespread tissue distribution, *i.e.* endophilin B1a, as well as a tissue-specific distribution such as the brain-specific variants endophilin B1b and B1c (Fig. 1). Although the widespread tissue distribution of

endophilin B1a is consistent with a role of endophilin B1 in ubiquitous membrane dynamics, our data do not exclude an involvement of the brain-specific endophilin B1 variants B1b and B1c in cell type-specific membrane dynamics such as those at synapses, which have been reported to show endophilin B1 immunoreactivity (15). Whatever the precise function of the endophilins B will be, it is likely to be an essential one, because the endophilins B, like the endophilins A, are conserved from yeast to humans (6, 11, 12, 15, 21, 22).

REFERENCES

1. Sparks, A. B., Rider, J. E., Hoffman, N. G., Fowlkes, D. M., Quilliam, L. A., and Kay, B. K. (1996) *Proc. Natl. Acad. Sci. U. S. A.* **93,** 1540–1544
2. Ringstad, N., Nemoto, Y., and De Camilli, P. (1997) *Proc. Natl. Acad. Sci. U. S. A.* **94,** 8569–8574
3. de Heuvel, E., Bell, A. W., Ramjaun, A. R., Wong, K., Sossin, W. S., and McPherson, P. S. (1997) *J. Biol. Chem.* **272,** 8710–8716
4. Giachino, C., Lantelme, E., Lanzetti, L., Saccone, S., Della Valle, G., and Migone, N. (1997) *Genomics* **41,** 427–434
5. Torrey, T., Kim, W., Morse, H. C., 3rd, and Kozak, C. A. (1998) *Mamm. Genome* **9,** 74–75
6. Huttner, W. B., and Schmidt, A. (2000) *Curr. Opin. Neurobiol.* **10,** 543–551
7. Schmidt, A., and Huttner, W. B. (1998) *Methods: A Companion to Methods Enzymol.* **16,** 160–169
8. Schmidt, A., Wolde, M., Thiele, C., Fest, W., Kratzin, H., Podtelejnikov, A. V., Witke, W., Huttner, W. B., and Söling, H.-D. (1999) *Nature* **401,** 133–141
9. Ringstad, N., Gad, H., Löw, P., Di Paolo, G., Brodin, L., Shupliakov, O., and De Camilli, P. (1999) *Neuron* **24,** 143–154
10. Gad, H., Ringstad, N., Low, P., Kjaerulff, O., Gustafsson, J., Wenk, M., Di Paolo, G., Nemoto, Y., Crun, J., Ellisman, M. H., De Camilli, P., Shupliakov, O., and Brodin, L. (2000) *Neuron* **27,** 301–312
11. Guichet, A., Wucherpfennig, T., Dudu, V., Etter, S., Wilsch-Bräuniger, M., Hellwig, A., González-Gaitán, M., Huttner, W. B., and Schmidt, A. A. (2002) *EMBO J.* **21,** 1661–1672
12. Verstreken, P., Kjaerulff, O., Lloyd, T. E., Atkinson, R., Zhou, Y., Meinerzhagen, I. A., and Bellen, H. J. (2002) *Cell* **109,** 101–112
13. Micheva, K. D., Ramjaun, A. R., Kay, B. K., and McPherson, P. S. (1997) *FEBS Lett.* **414,** 308–312
14. Slepnev, V. I., and De Camilli, P. (2000) *Nat. Rev. Neurosci.* **1,** 161–172
15. Farsad, K., Ringstad, N., Takei, K., Floyd, S. R., Rose, K., and De Camilli, P. (2001) *J. Cell Biol.* **155,** 193–200
16. Huttner, W. B., and Schmidt, A. A. (2002) *Trends Cell Biol.* **12,** 155–158
17. Simpson, F., Hussain, N. K., Qualmann, B., Kelly, R. B., Kay, B. K., McPherson, P. S., and Schmid, S. L. (1999) *Nat. Cell Biol.* **1,** 119–124
18. Howard, L., Nelson, K. K., Maciewicz, R. A., and Blobel, C. P. (1999) *J. Biol. Chem.* **274,** 31693–31699
19. Tang, Y., Hu, L. A., Miller, W. E., Ringstad, N., Hall, R. A., Pitcher, J. A., De Camilli, P., and Lefkowitz, R. J. (1999) *Proc. Natl. Acad. Sci. U. S. A.* **96,** 12559–12564
20. Ochoa, G. C., Slepnev, V. I., Neff, L., Ringstad, N., Takei, K., Daniell, L., Kim, W., Cao, H., McNiven, M., Baron, R., and De Camilli, P. (2000) *J. Cell Biol.* **150,** 377–389
21. Pierrat, B., Simonen, M., Cueto, M., Mestan, J., Ferrigno, P., and Heim, J. (2001) *Genomics* **71,** 222–234
22. Cuddeback, S. M., Yamaguchi, H., Komatsu, K., Miyashita, T., Yamada, M., Wu, C., Singh, S., and Wang, H. G. (2001) *J. Biol. Chem.* **276,** 20559–20565
23. Altschul, S. F., Madden, T. L., Schaffer, A. A., Zhang, J., Zhang, Z., Miller, W., and Lipman, D. J. (1997) *Nucleic Acids Res.* **25,** 3389–3402
24. Ausubel, F., Brent, R., Kingston, R. E., Moore, D. D., Seidman, J. G., Smith, J. A., and Struhl, K. (1997) *Short Protocols in Molecular Biology*, 3rd. Ed., John Wiley & Sons Inc., New York
25. Gray, E. G., and Whittaker, V. P. (1962) *J. Anat.* **96,** 79–86
26. Balch, W. E., Dunphy, W. G., Braell, W. A., and Rothman, J. E. (1984) *Cell* **39,** 405–416
27. Modregger, J., Ritter, B., Witter, B., Paulsson, M., and Plomann, M. (2000) *J. Cell Sci.* **113,** 4511–4521
28. Plomann, M., Lange, R., Vopper, G., Cremer, H., Heinlein, U. A. O., Scheff, S., Baldwin, S. A., Leitges, M., Cramer, M., Paulsson, M., and Barthels, D. (1998) *Eur. J. Biochem.* **256,** 201–211
29. Qualmann, B., Roos, J., DiGregorio, P. J., and Kelly, R. B. (1999) *Mol. Biol. Cell* **10,** 501–513
30. Kozak, M. (1991) *J. Cell Biol.* **115,** 887–903
31. Sittler, A., Walter, S., Wedemeyer, N., Hasenbank, R., Scherzinger, E., Eickhoff, H., Bates, G. P., Lehrach, H., and Wanker, E. E. (1998) *Mol. Cell* **2,** 427–436
32. Cremona, O., Di Paolo, G., Wenk, M. R., Lüthi, A., Kim, W. T., Takei, K., Daniell, L., Nemoto, Y., Shears, S. B., Flavell, R. A., McCormick, D. A., and De Camilli, P. (1999) *Cell* **99,** 179–188
33. Hilfiker, S., Pieribone, V. A., Czernik, A. J., Kao, H. T., Augustine, G. J., and Greengard, P. (1999) *Philos. Trans. R. Soc. Lond. B. Biol. Sci.* **354,** 269–279
34. Cao, H., Garcia, F., and McNiven, M. A. (1998) *Mol. Biol. Cell* **9,** 2595–2609
35. Jones, S. M., Howell, K. E., Henley, J. R., Cao, H., and McNiven, M. A. (1998) *Science* **279,** 573–577
36. DiFiglia, M., Sapp, E., Chase, K., Schwarz, C., Meloni, A., Young, C., Martin, E., Vonsattel, J. P., Carraway, R., and Reeves, S. A. (1995) *Neuron* **14,** 1075–1081
37. Wood, J. D., MacMillan, J. C., Harper, P. S., Lowenstein, P. R., and Jones, A. L. (1996) *Hum. Mol. Genet.* **5,** 481–487
38. Velier, J., Kim, M., Schwarz, C., Kim, T. W., Sapp, E., Chase, K., Aronin, N., and DiFiglia, M. (1998) *Exp. Neurol.* **152,** 34–40